Electronic Supplementary Material (ESI) for Polymer Chemistry.
This journal is © The Royal Society of Chemistry 2014

Polymer Chemistry RSCPublishing

SUPPORTING INFORMATION

Branched Polythiophenes by Ni-Catalyzed Kumada Coupling

Martin Scheuble,[a] Thomas V. Richter,[a] Miriam Goll,[a] Steffen Link[a], Juan T. López Navarrete,[b] Adrian Ruff,[a] M. Carmen Ruiz Delgado,[b] and Sabine Ludwigs[a,]*

doi: 10.1039/C4PY00899E

I Synthesis and Characterization.

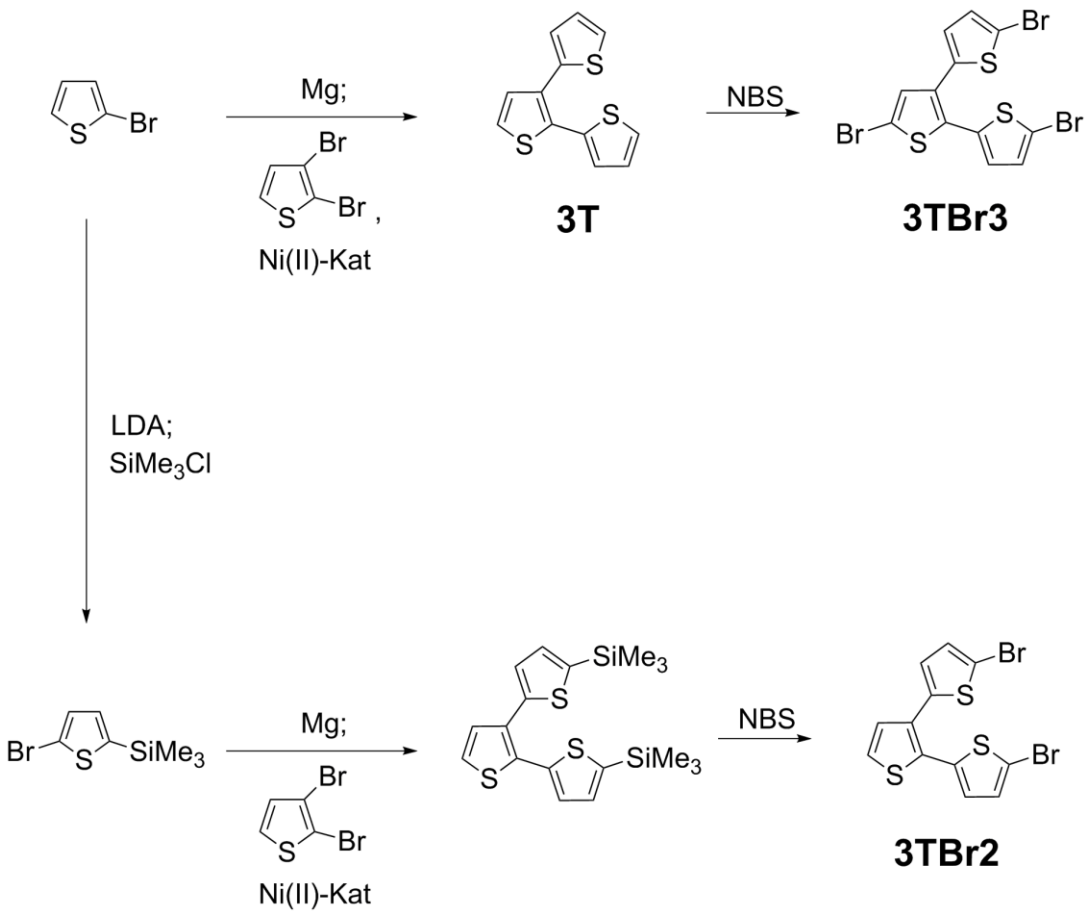

Fig. S1: Synthesis of monomers **3TBr3** (top) and **3TBr2** (bottom).

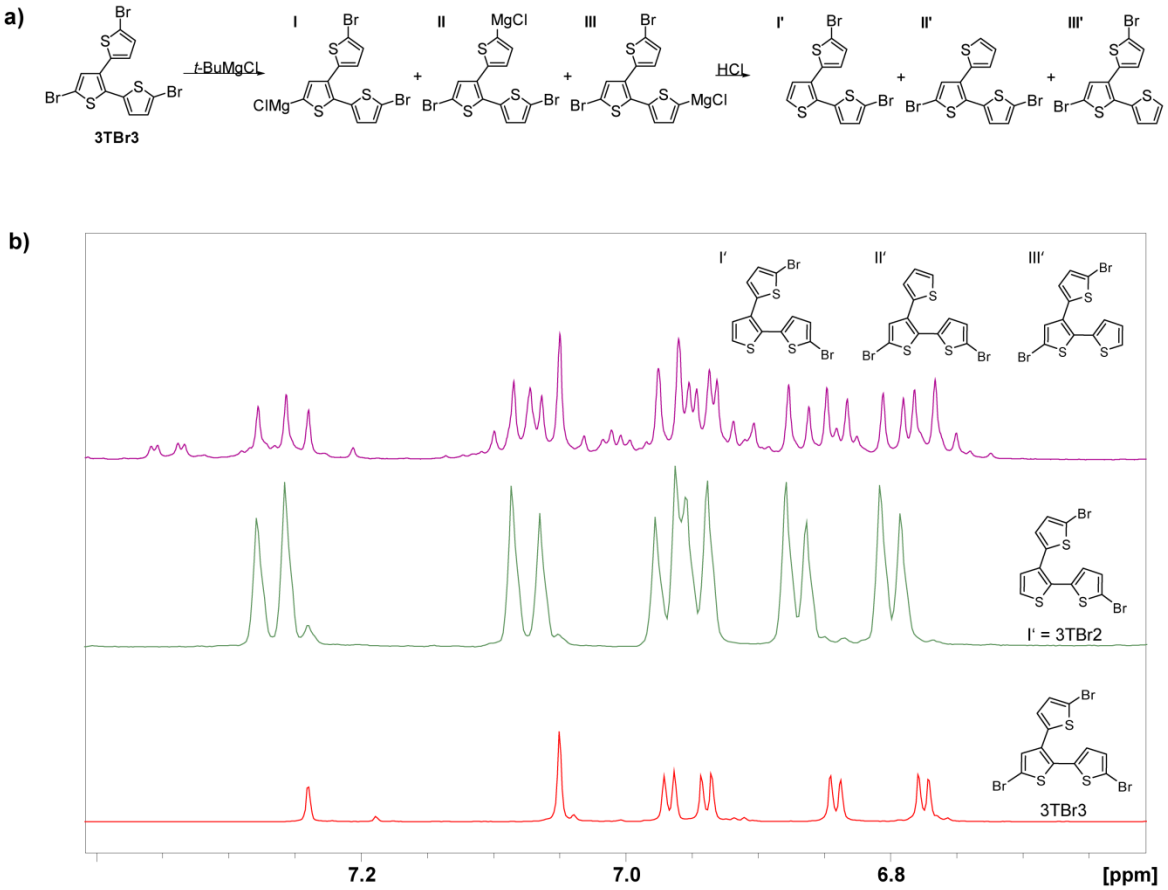

Fig. S2: Quenching experiments: a) synthetic route for quenching experiment starting from **3TBr3** b) comparison of ^{1}H-NMR spectra of **3TBr3** (starting material), **3TBr2** (seperatly synthesized) and quenched monomermixture.

 This journal is © The Royal Society of Chemistry 2014

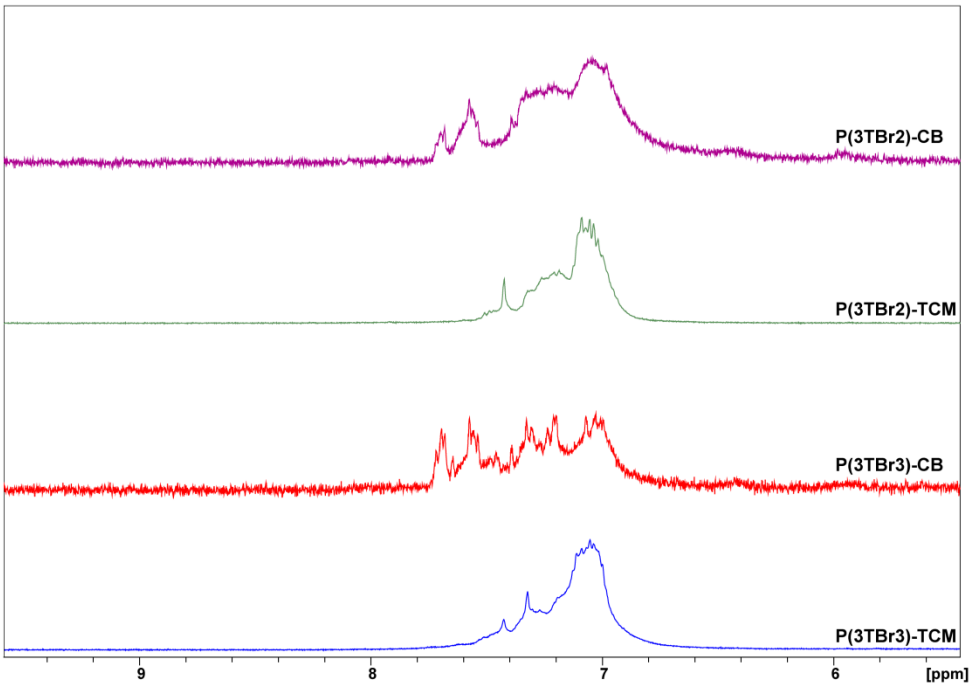

Fig. S3: ^{1}H-NMR spectra (250 MHz, d8-THF) of different **P(3TBrX)** fractions.

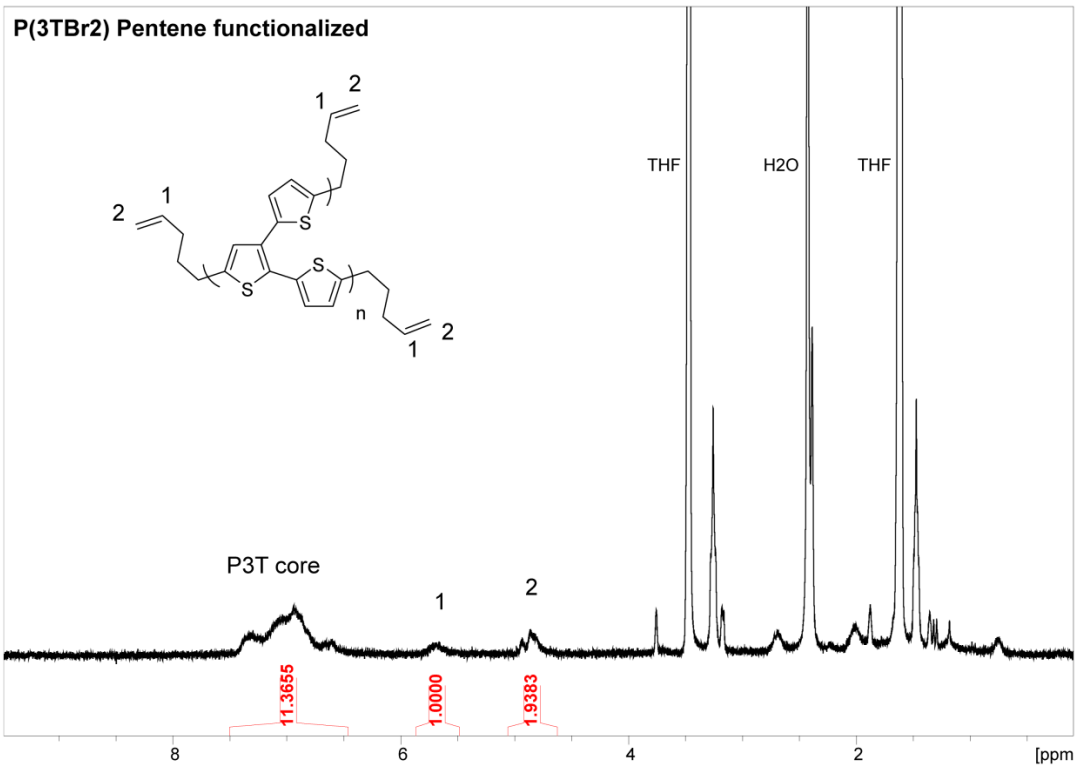

Fig. S4: ^{1}H-NMR (250 MHz, THF-d8) of pentene functionalized **P(3TBr2).**

 This journal is © The Royal Society of Chemistry 2014

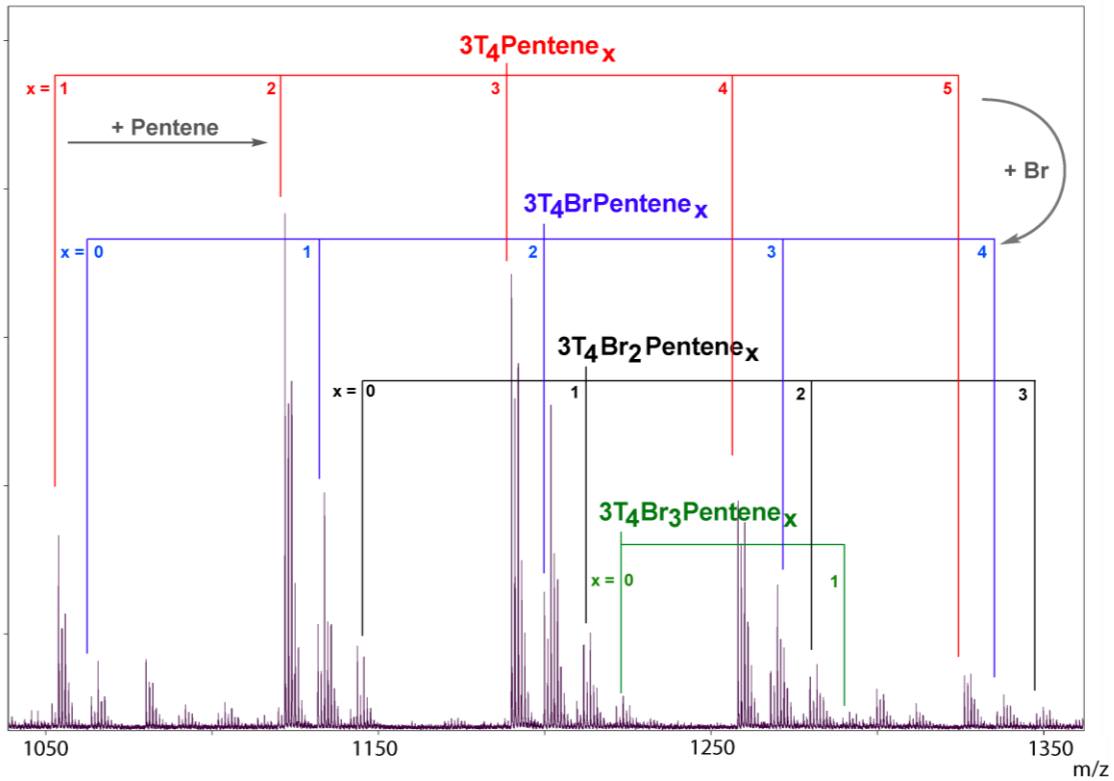

Fig. S5: Representative MALDI-TOF spectra of pentene functionalized, branched **P(3TBr2).** All intense peaks in the MALDI-TOF spectrum can be assigned to functionalized branched polythiophene species. All species bear either H-, Br- or pentene endgroups in α-position, so that the species present in the spectra can be represented by the formula $3T_yBr_zPentene_x$. Fig. S5 shows the peaks that can be assigned to the 3T-tetramer ($3T_4$). The main distribution in the spectra can be assigned to species with only pentene and H-endgroups, where the difference between the signals is one pentene group. Different subdistributions can be identified and assigned to the series with $3T_4Br_1Pentene_x$, $3T_4Br_2Pentene_x$ and so on.

Rough calculation of the degree of functionalization: Based on the obtained MALDI-TOF spectra the intensities of the single signals of the isotopic pattern for one 3TNBrN+2-XHX species were added up and multiplied with the functionalization degree of this species ((N+2-X)/(N+2)). These numbers were added up and divided by the sum of all intensities for all peaks of this degree of polymerization and rounded to the nearest tens. The obtained value can only be seen as a rough estimation, because intensities and not peak areas were taken into account (because of the high noise level) and the discrimination of higher molecular weight by MALDI-TOF experiments.

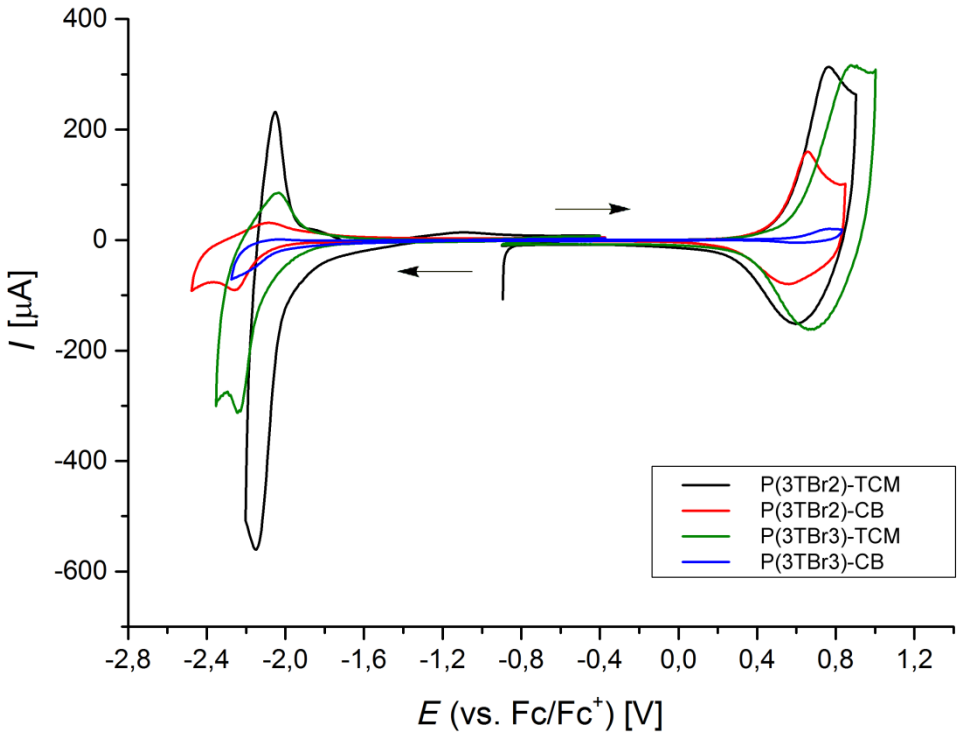

Fig. S6: Cyclic voltammograms of **P(3TBrX)**. Films obtained by drop-casting on gold electrodes. Measurements were performed in MeCN, 0.1 M NBu_4PF_6, 20 mV/s except for the reduction of **P(3TBr3)-CB** where it was 50 mV/s. Oxidation and reduction cycles were measured separately. Smaller current of **P(3TBr3)-CB** is ascribed to a thinner film. Ferrocene / ferrocenium was used as external standard.

 This journal is © The Royal Society of Chemistry 2014

II Computational details.

The molecular geometries of different 3T-based oligomeric models were calculated at the Density Functional Theory (DFT) level using the hybrid, generalized gradient approximation (GGA) functional B3LYP[1,2] and a 6-31G** basis[3–5] set, as implemented in the GAUSSIAN09 program.[6] Note that the final shape of the oligomer (*i.e.*, branching density) can be highly dependent on the choice of the orientation of the 3T monomer and number of repeating 3T units. In this work, in order to simulate architectures with different branching densities, different orientations of the 3T monomer were considered and the 3T units were built in in a random or regular fashion (the models considered are denoted as **L**, **B**, **L-1b**, **L-3b**, see Figure S7). The more recently developed long-range corrected Coulomb attenuated method of B3LYP (CAM-B3LYP functional)[7] was also used to evaluate the oligomer ground-state geometries. In general, the results (*i.e.*, twist angles between thienyl untis, see Figures S8-S12 in the Supporting Information) were very similar when compared to those obtained at the B3LYP level. All geometrical parameters were allowed to vary independently apart from planarity of the rings and no symmetry constraints were imposed during the optimization process. On the resulting ground-state optimized geometries, harmonic frequencies calculations were performed to ensure the finding of the global minimum. Vertical electronic excitation energies were computed by using the time-dependent DFT (TD-DFT) approach on the previously optimized molecular geometries. CAM-B3LYP functional was also employed to examine the excited-state properties. The $S_0 \rightarrow S_1$ transition energies calculated at the CAM-B3LYP level were moderately blue shifted when compared to those calculated at the B3LYP level. However, very similar trends in the orbital description and in the evolution of the electronic absorption spectra within the series were found for both B3LYP and CAM-B3LYP functionals. Absorption spectra were simulated through convolution of the vertical transition energies and oscillator strengths with Gaussian functions characterized by a half width at half-maximum (fwhm) of 0.3 eV. Molecular orbital contours were plotted using gausview 5.0. The geometry of the radical cation of 3T was optimized in order to calculate the Mulliken atomic spin densities.

Comments on the oligomeric models considered in DFT calculations:

Density functional theory (DFT) calculations were carried out on the following oligomeric models (see Figure S7): (i) five repeating 3T units α,α-connected in a regioregular fashion (i.e., named as **L**) as models for the more linear 3T-based polymers, and (ii) five repeat 3T units α,α-connected in regiorandom fashion (*i.e.*, named as **B**) and an extension of the linear pentamer **L** with one and three additional 3T units (*i.e.*, named as **L-1b** and **L-3b**) as models for the more branched **3T**-based polymers. These models will allow us to investigate the influence of the orientation and number of 3T repeating units (and thus, the branching density) on the optical and electronic properties of resulting branched polythiophenes.

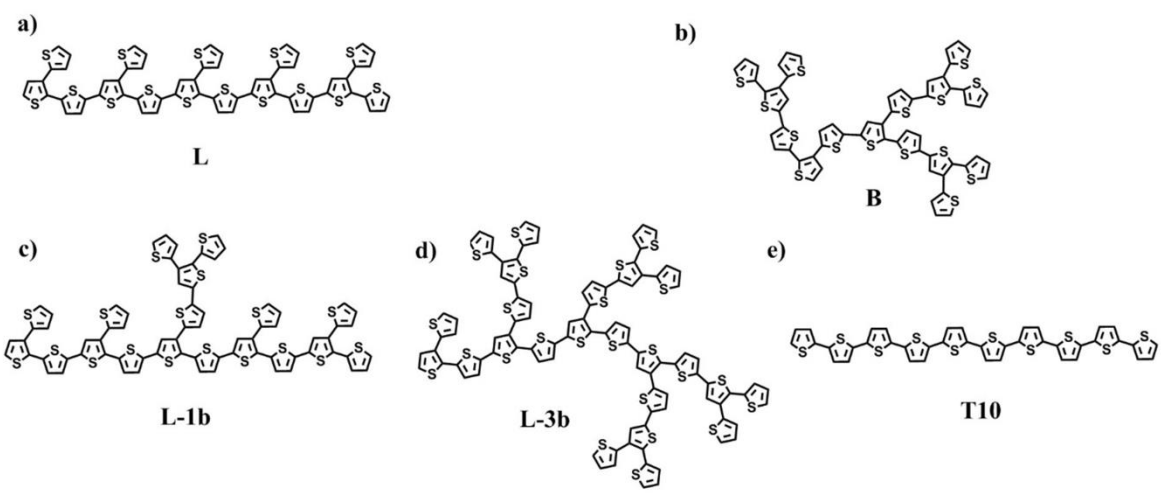

Figure S7. Chemical structures of the 3T-based model systems studied theoretically: (a) linear pentamer **L**, (b) branched pentamer **B,** (c) linear pentamer with one branched unit **L-1b,** (d) linear pentamer with three branched units **L-3b** and e) linear unsubstituted decamer **T10.** Note that **L** can be used as model for the more linear polymers *(i.e.*, **P(3T)**) and **B**, **L-1b** and **L-3b** as models for the more branched polymers (*i.e.*, **P(3TBrX)** polymers).

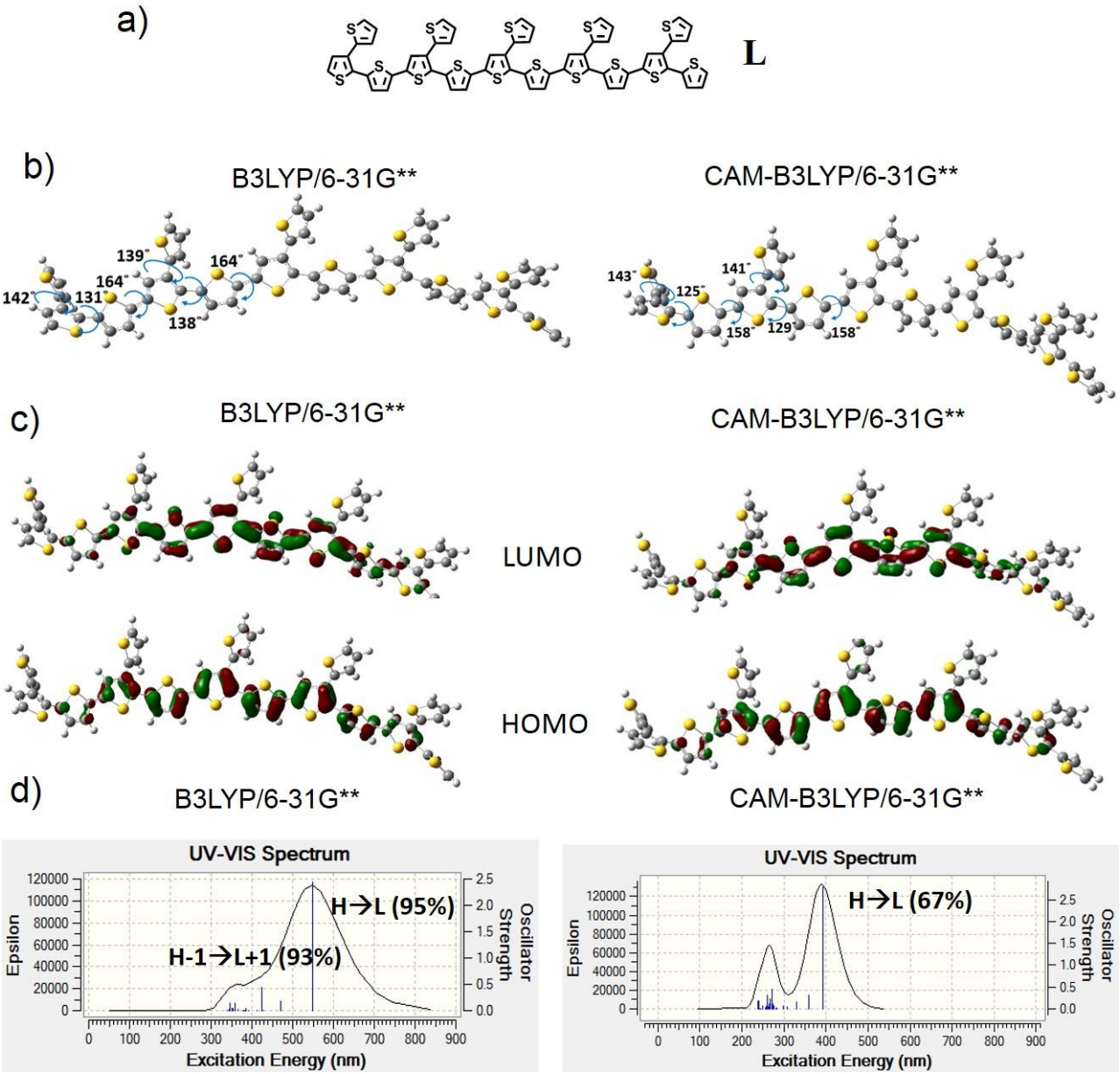

Figure S8. a) Chemical structure of model system **L**. b) Thiophene–thiophene dihedral angles. c) HOMO and LUMO wave functions. d) Simulated absorption spectra together with the excitations (wavelength vs. oscillator strength) shown as vertical bars as determined with TD-DFT.

 This journal is © The Royal Society of Chemistry 2014

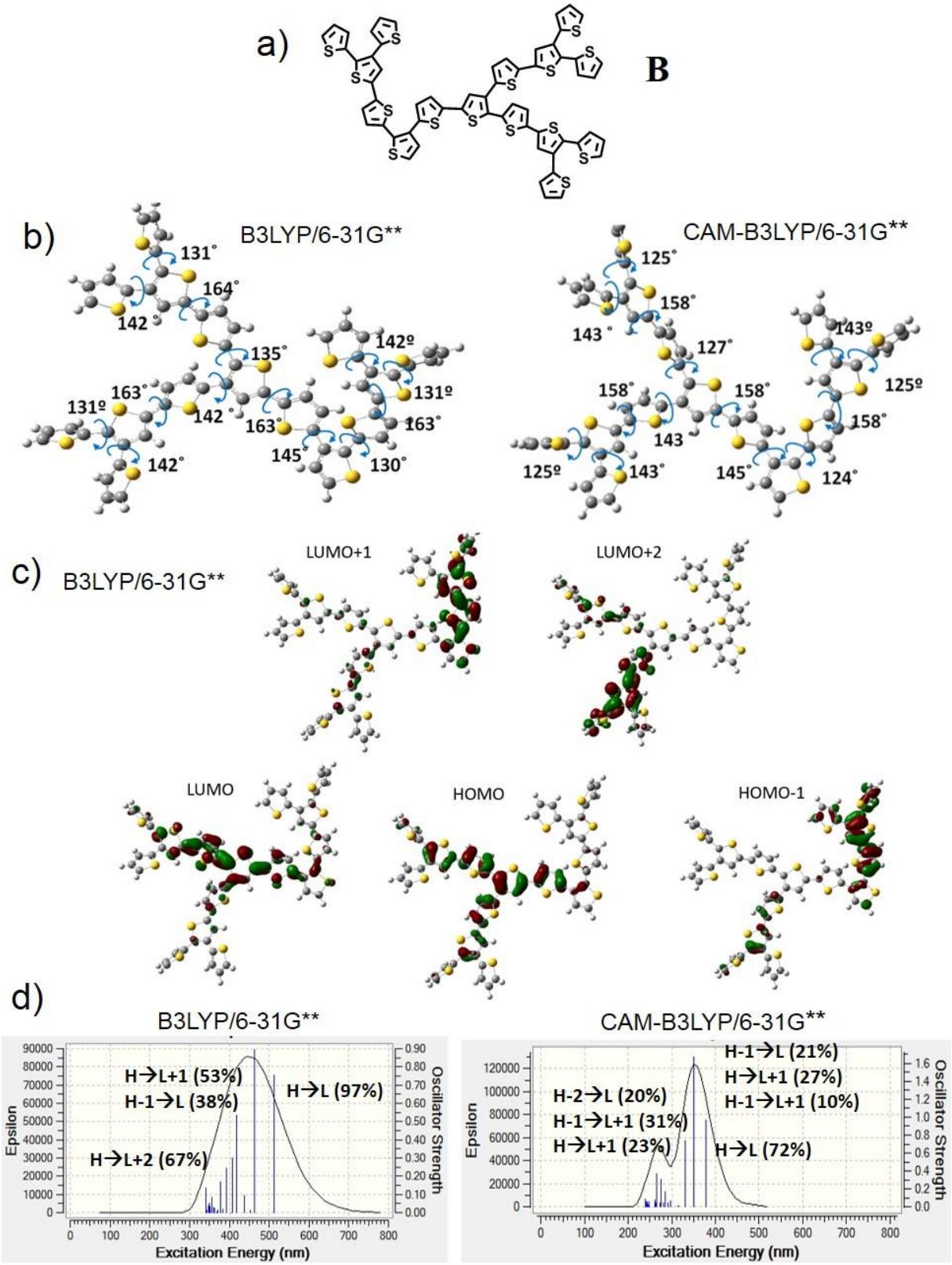

Figure S9. a) Chemical structure of model system **B**. b) Thiophene–thiophene dihedral angles. c) Topologies of the molecular orbitals involved in the most intense calculated vertical transitions. d) Simulated absorption spectra together with the excitations (wavelength vs. oscillator strength) shown as vertical bars as determined with TD-DFT. It can be observed that the absorption maxima for **B** are not due to the strongest transition but to the sum of some higher energy transitions that are very close in energy.

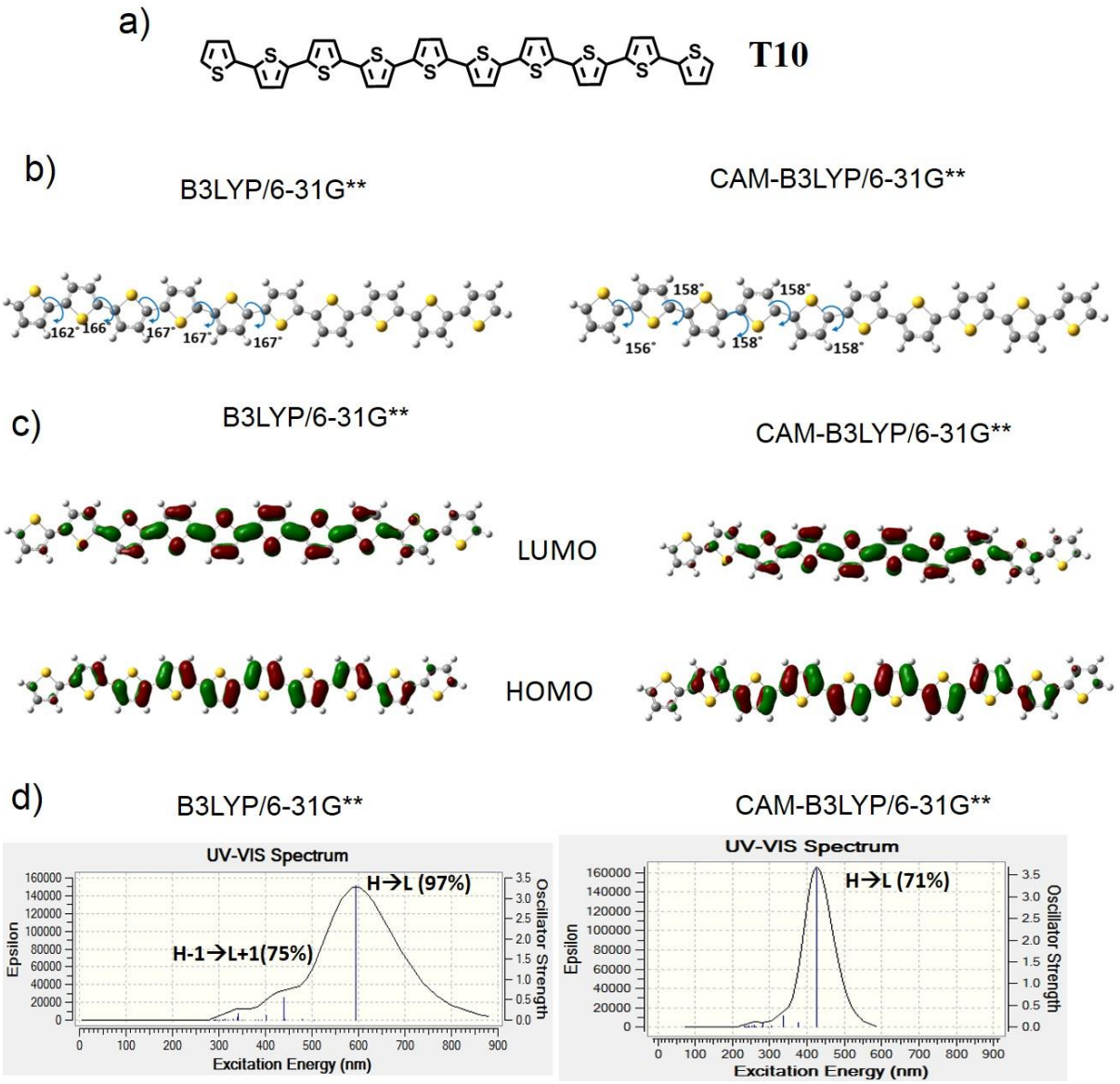

Figure S10. a) Chemical structure of model system **T10**. b) Thiophene−thiophene dihedral angles. c) Topologies of the molecular orbitals involved in the most intense calculated vertical transitions. d) Simulated absorption spectra together with the excitations (wavelength vs. oscillator strength) shown as vertical bars as determined with TD-DFT.

 This journal is © The Royal Society of Chemistry 2014

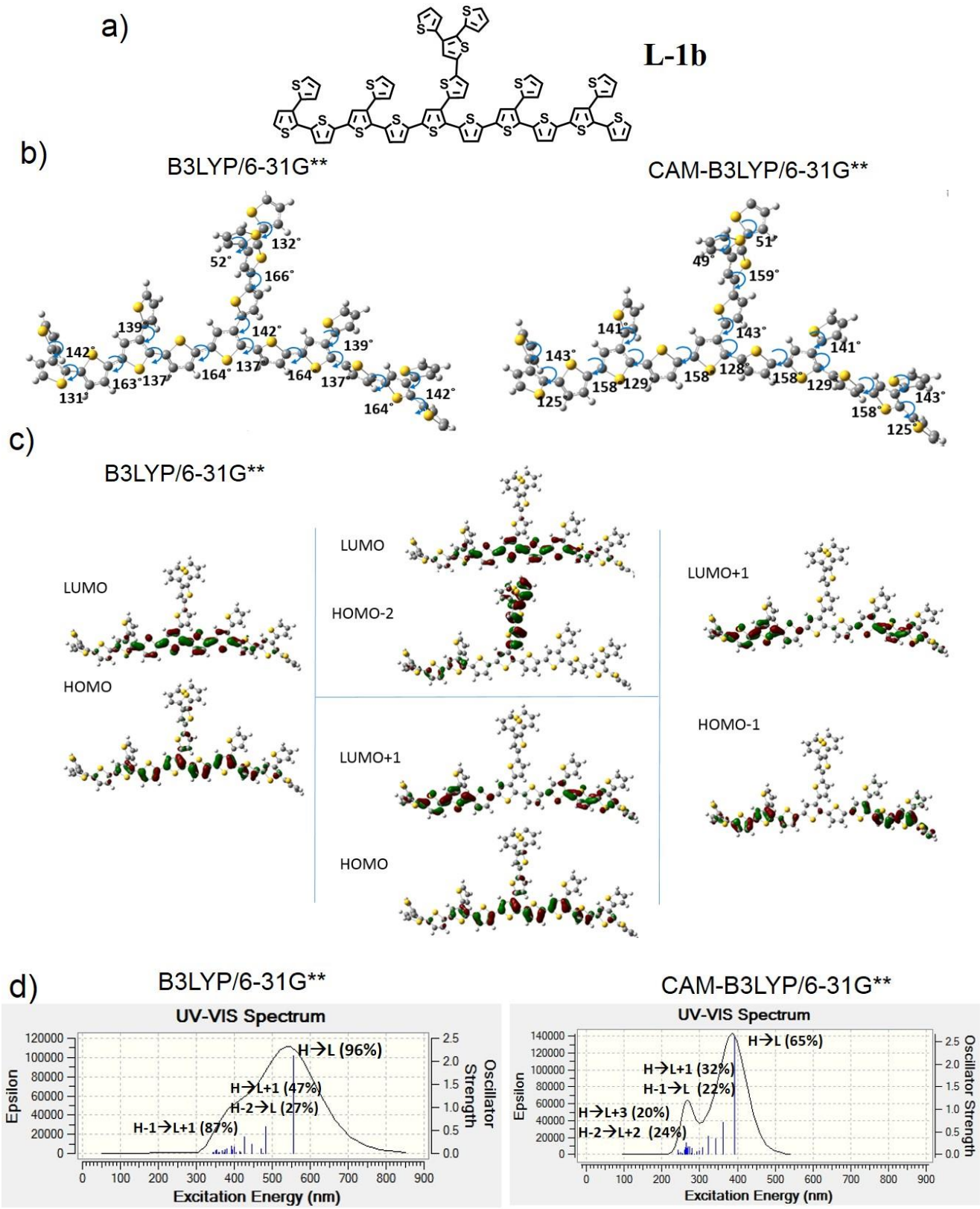

Figure S11. a) Chemical structure of model system **L-1b**. b) Thiophene−thiophene dihedral angles. c) Topologies of the molecular orbitals involved in the most intense calculated vertical transitions. d) Simulated absorption spectra together with the excitations (wavelength vs. oscillator strength) shown as vertical bars as determined with TD-DFT.

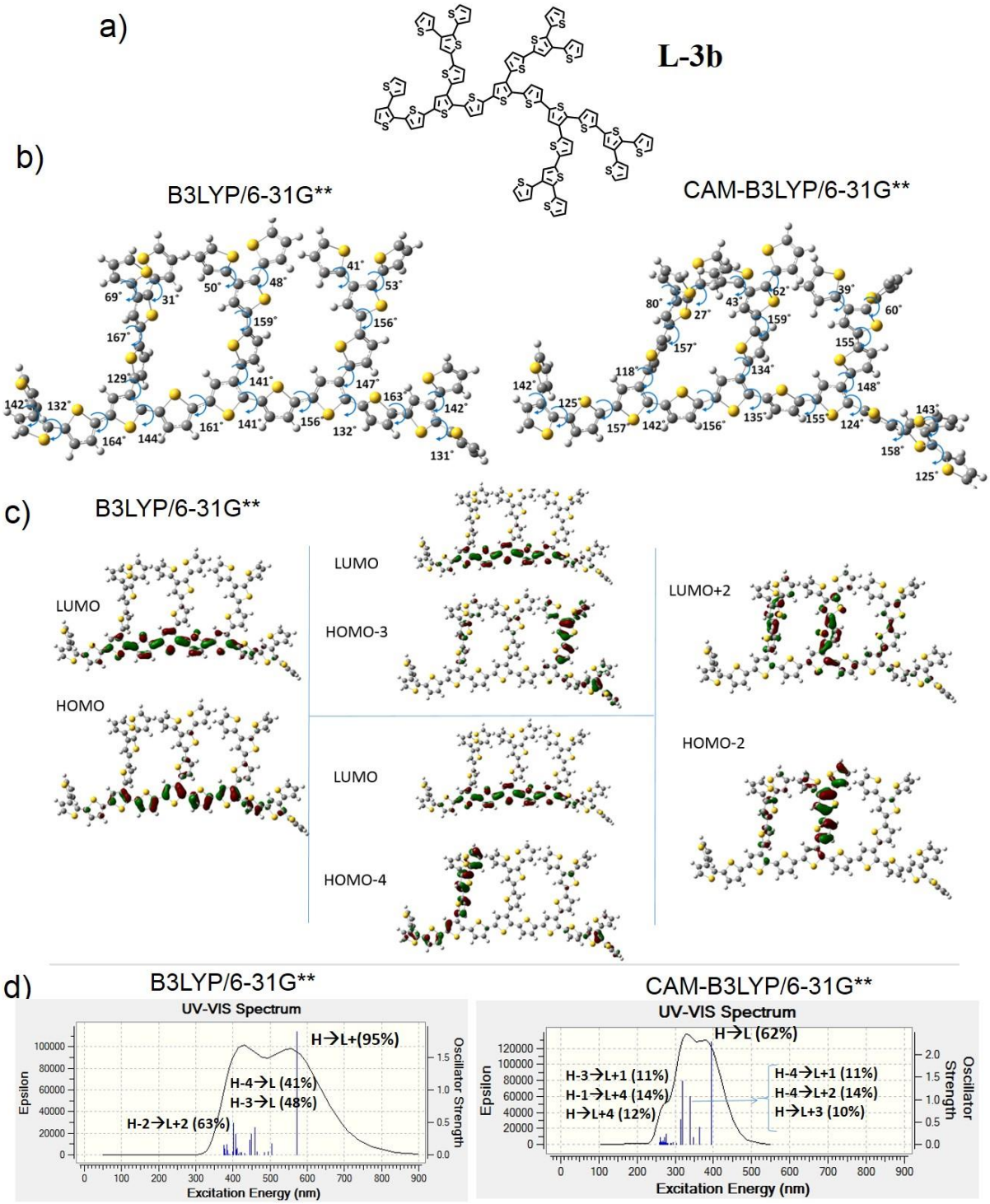

Figure S12. a) Chemical structure of model system **L-3b**. b) Thiophene−thiophene dihedral angles. c) Topologies of the molecular orbitals involved in the most intense calculated vertical transitions. d) Simulated absorption spectra together with the excitations (wavelength vs. oscillator strength) shown as vertical bars as determined with TD-DFT. An increase of the low energy band is observed when going from **L-1b** to **L-3b** (i.e., when increasing the number of branched units) which is attributed to the presence of a larger number of energy transitions at higher energy.

 This journal is © The Royal Society of Chemistry 2014

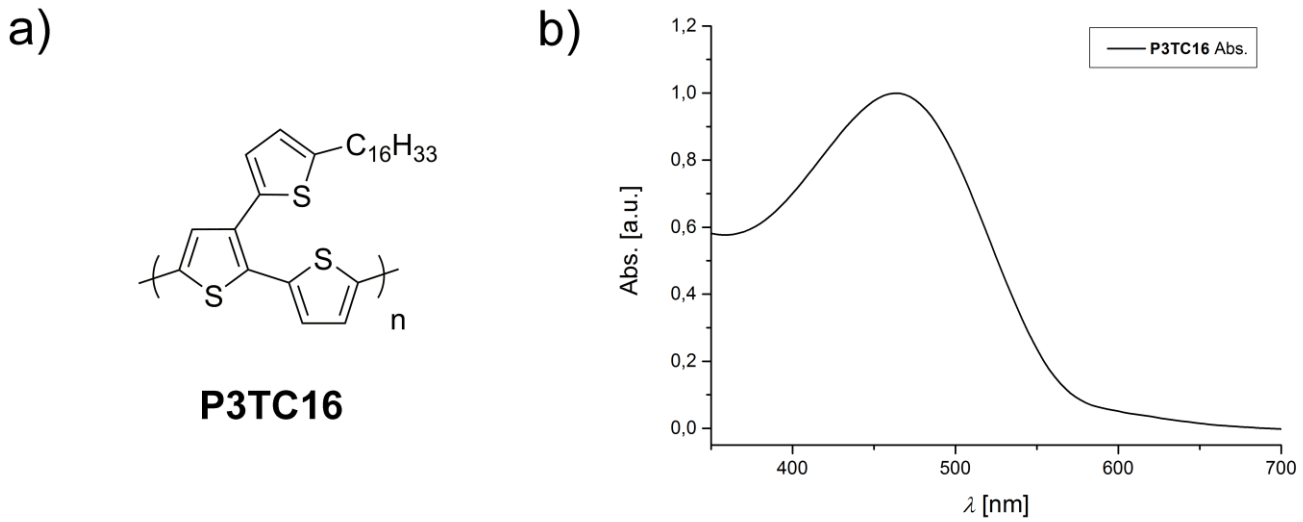

Figure S13. a) Chemical structure of sidechain π-extended polythiophene **P3TC16 b)** Absorption spectra of **P3TC16** in hot oDCB solution.

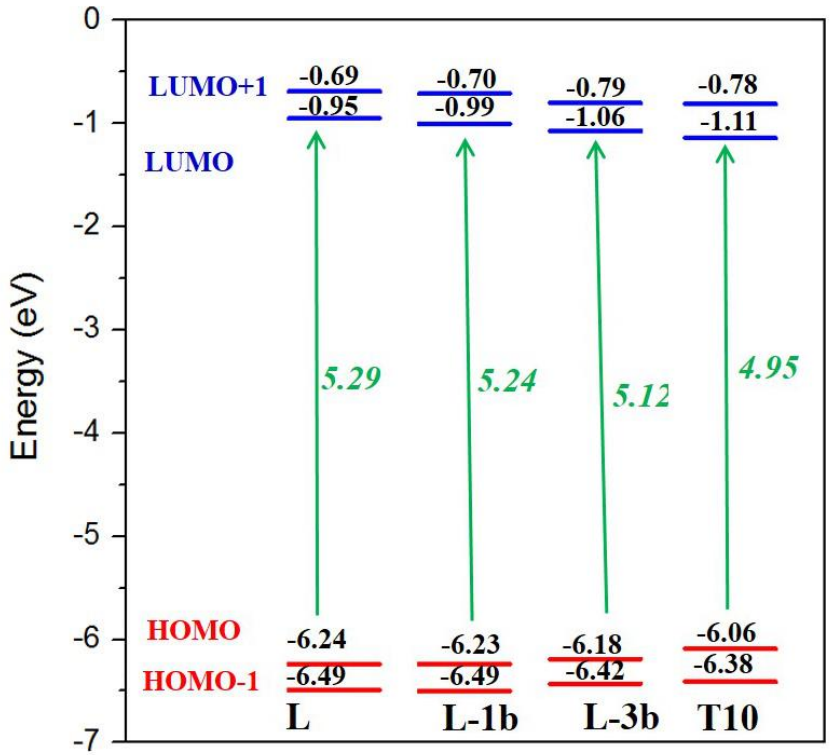

Figure S14. CAM-B3LYP/6–31G** absolute energy values for the molecular orbitals around the energy gap. Arrows denote the HOMO-LUMO gap.

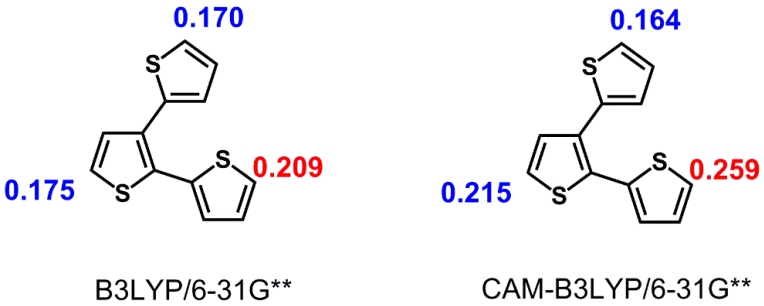

Figure S15 . Mulliken atomic spin densities at the terminal α-carbons of **3T** radical cation as determined at the B3LYP/6-31G** and CAM-B3LYP/6-31G** level of theory.

 This journal is © The Royal Society of Chemistry 2014

References.

1. A. D. Becke, *J. Chem. Phys.*, 1993, **98**, 5648.
2. C. Lee, W. Yang, and R. Parr, *Phys. Rev. B*, 1988, **37**, 785.
3. P. Hariharan and J. Pople, *Theor. Chim. Acta*, 1973, **28**, 213–222.
4. W. J. Hehre, R. Ditchfield, and J. A. Rople, *J. Chem. Phys.*, 1972, **56**, 2257.
5. M. M. Francl, *J. Chem. Phys.*, 1982, **77**, 3654.
6. M. J. Frisch et al., Gaussian 09, revision B.01: Pittsburgh, PA, 2009.
7. T. Yanai, D. P. Tew, and N. C. Handy, *Chem. Phys. Lett.*, 2004, **393**, 51–57.